Materials Letters 174 (2016) 188–191

Contents lists available at ScienceDirect

Materials Letters

journal homepage: www.elsevier.com/locate/matlet

Chemical vapor deposition of ultra-thin molybdenum dioxide nanosheets

Jidong Li, Jun Yin, Xuemei Li, Jianxin Zhou, Wanlin Guo *

State Key Laboratory of Mechanics and Control of Mechanical Structures, Key Laboratory for Intelligent Nano Materials and Devices of the Ministry of Education, Institute of Nanoscience, Nanjing University of Aeronautics and Astronautics, 29 Yudao Street, Nanjing 210016, China

ARTICLE INFO

Article history:
Received 4 September 2015
Received in revised form
21 February 2016
Accepted 14 March 2016
Available online 15 March 2016

Keywords:
Crystal growth
Chemical vapor deposition
Molybdenum dioxide
Molybdenum trioxide
Electrical properties

ABSTRACT

We report the growth of ultra-thin molybdenum dioxide nanosheets on SiO_2/Si substrate via chemical vapor deposition using molybdenum trioxide and sublimated sulfur as precursors. The thicknesses of the obtained MoO_2 nanosheets show notable dependence on the baking temperature of the sulfur precursor. At sulfur temperature of 90 °C, the obtained nanosheets can be 5.5 nm thin, more than one order of magnitude thinner than that previously reported, in a narrow scatter ranging from 5.5 to 11.5 nm. Two-probe electrical measurements show that the as-prepared ultrathin MoO_2 nanosheets preserve a high electrical conductivity of 3600 S/cm with thermal stability up to 200 °C. Above 250 °C, metallic MoO_2 nanosheets are oxidized into insulating MoO_3 flakes in air.

1. Introduction

Two dimensional (2D) semiconducting molybdenum dichalcogenides have attracted intensive interest for their atomic layered structure with excellent electrical properties. However, electrical contact to these 2D semiconductors remains a great challenge for the Femi level pinning effect at the metal–semiconductor junction [1]. Molybdenum oxides (MoO_x), as a material of high work function material, has been demonstrated to exhibit promising contact to MoS_2 or WSe_2 based field-effect transistors and diodes because of the efficient hole-injection and lower degree of interface Femi-level pinning [2]. Moreover, an enhanced electrical connection is also observed in organic light-emitting diodes when using ultrathin layer of molybdenum dioxide (MoO_2) with thicknesses ranging from 0.25 to 10 nm as buffer layer [3]. Although MoO_x is a promising electrode material, the preparation of highly conductive 2D MoO_x with thickness less than 10 nm has not been achieved.

Previously, MoO_2 nanosheets have been prepared via a hydrothermal method [4]. But the complex nanostructure and rich defects of MoO_2 resulting from hydrothermal reduction would severely limit its application in devices. Chemical vapor deposition (CVD), as a well-established method to grow high-quality 2D crystals, has been successfully employed to synthesize MoO_2 or MoO_3 flakes [5–8]. Reduced by sulfur vapor, MoO_3 powder can be thermally evaporated and deposited as MoO_2 flakes on the Si/SiO_2 substrate [9]. Through this method, Wang et al. have prepared high-quality MoO_2 microplates as templates for the growth of highly crystalline MoS_2 layers [5]. But these MoO_2 microplates are commonly thicker than 100 nm, far from the desired thickness less than 10 nm. Nanosheets prepared by Hao show thickness down to 15 nm but in very poor quality as indicated by the Raman spectrum where several typical peaks of the MoO_2 crystalline are even absent [6].

Here we report CVD growth of MoO_2 nanosheets with both high crystallinity and ultrathin thickness down to 5.5 nm. Moderate sublimation of sulfur precursor is crucial for the growth of high-quality MoO_2 nanosheets. The obtained MoO_2 flakes preserve high electrical conductivity with heat resistance up to 200 °C. These outstanding performances indicate MoO_2 to be a promising candidate in the area of nanoelectronics.

2. Materials and methods

The ultrathin MoO_2 flakes were synthesized on substrate of Si with 285 nm of SiO_2 via CVD process. As illustrated in Fig. 1a, the SiO_2/Si substrate cleaned by piranha solution (sulfuric acid:hydrogen peroxide=3:1) was loaded into the center of a 2-inch furnace and placed face-down above a ceramic crucible with 10 mg of MoO_3 powder (Ourchem, 99.99%) inside. Another

* Corresponding author.
E-mail address: wlguo@nuaa.edu.cn (W. Guo).

http://dx.doi.org/10.1016/j.matlet.2016.03.081
0167-577X/

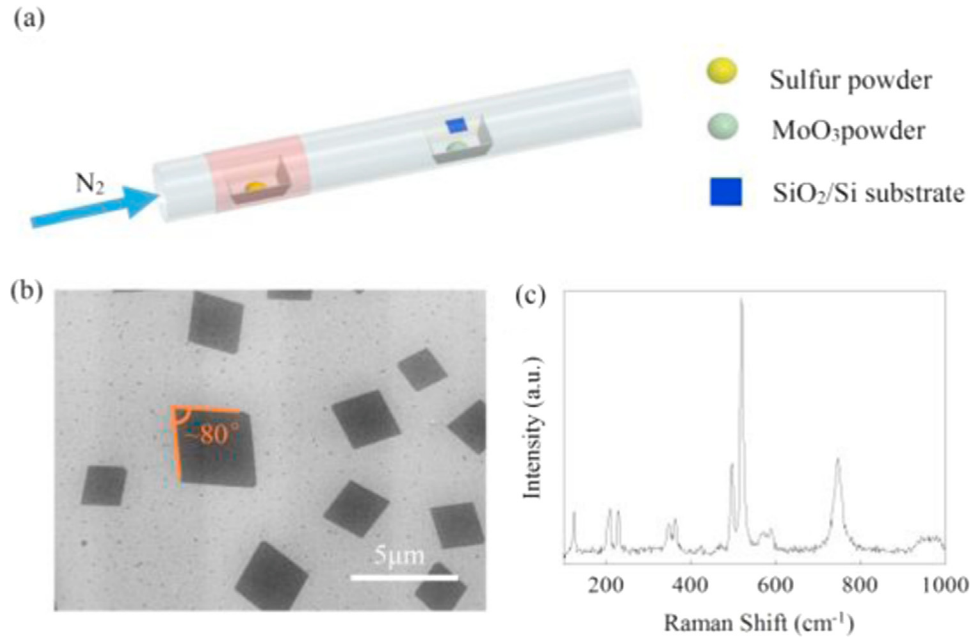

Fig. 1. Growth and characterization of ultrathin MoO_2 nanosheets. (a) Schematic diagram of the CVD system for MoO_2 synthesis. The temperature of sulfur powder is controlled by a heating belt (red region). (b) SEM image of MoO_2 nanosheets grown on SiO_2/Si substrate. (c) Typical Raman spectrum of a MoO_2 nanosheet. (For interpretation of the references to color in this figure legend, the reader is referred to the web version of this article.)

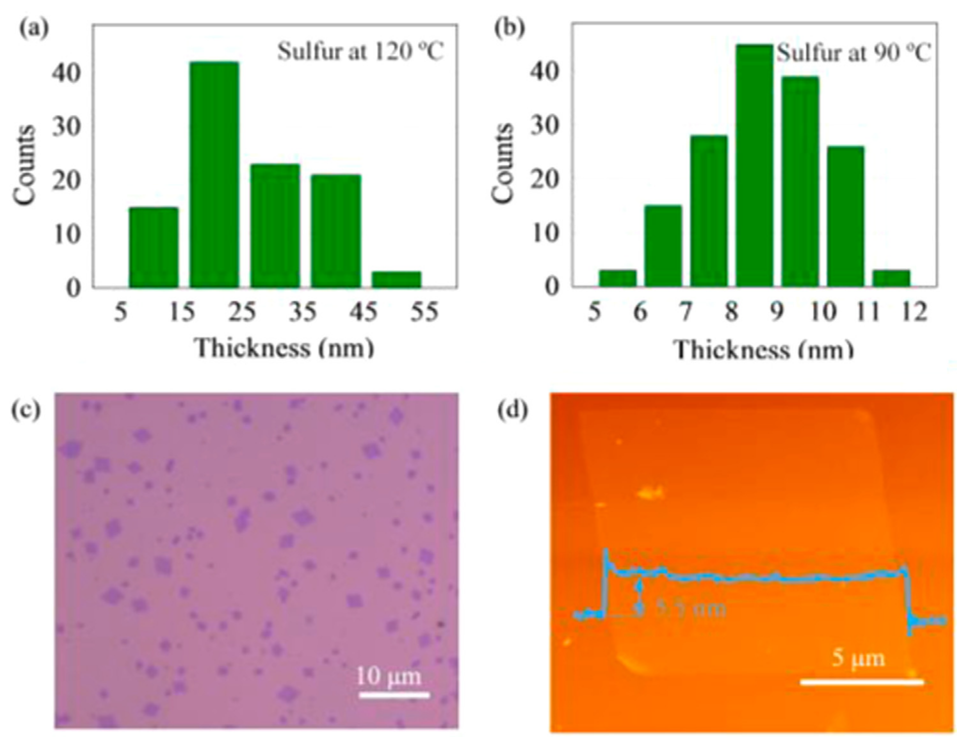

Fig. 2. Dependence of flake thickness on the temperature of sulfur. (a, b) Thickness distribution of MoO_2 flakes grown at a sulfur temperature of 120 °C (a) and 90 °C (b), respectively. (c) Optical microscopy image of the MoO_2 flakes grown on SiO_2/Si substrate at sulfur temperature of 90 °C. (d) AFM image of an ultrathin MoO_2 nanosheet and the height profile.

crucible with 100 mg of sulfur powder (Alfa Aesar, 99.5%) was placed upstream. The furnace was heated to 750 °C in 30 min with a flow of 10 sccm nitrogen gas, and the temperature of sulfur was controlled at desired temperature by a heating belt. After growth at 750 °C for 10 min, the furnace was cooled slowly down to 600 °C without feedback. Finally, the N_2 flow was set to 100 sccm before the sulfur source and the furnace were cooled to ambient temperature rapidly. The Raman spectra was conducted by a Renishaw Raman spectrometer with a 532 nm solid-state laser. The devices were fabricated by standard electron-beam lithography, thermal evaporation of ~60 nm Au electrodes, and final lift-off. The voltage was loaded on the devices and the current was

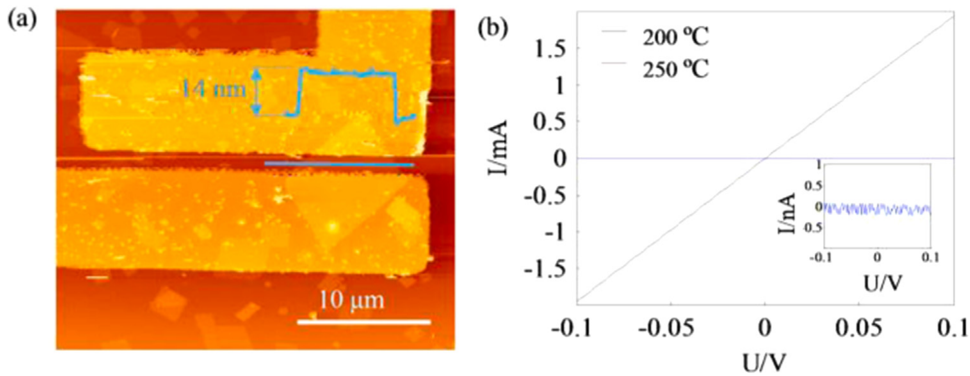

Fig. 3. Electrical properties of MoO_2. (a) AFM image of a device with patterned electrodes. The height profile along the blue line shows the thickness of the MoO_2 is around 14 nm. (b) I-V curves of two flakes measured at room temperature after annealed in air for half an hour at 200 °C and 250 °C, respectively. (For interpretation of the references to color in this figure legend, the reader is referred to the web version of this article.)

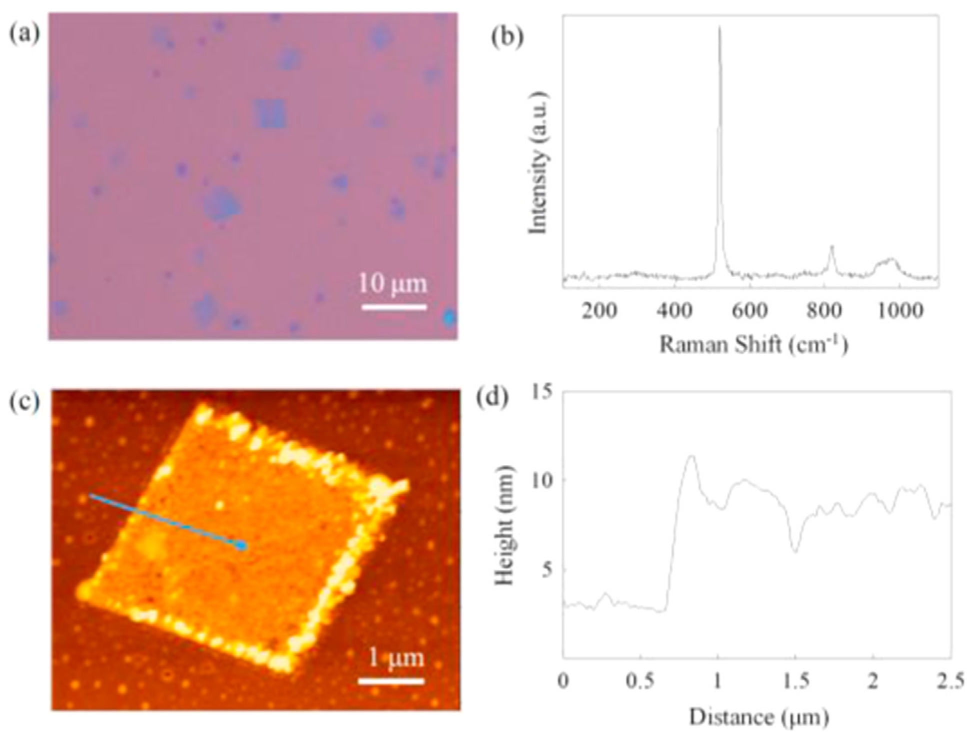

Fig. 4. Characterization of oxidized MoO_2 nanoflakes. (a) Optical microscopy image of the oxidized MoO_2 flakes. (b) Raman spectrum of the oxidized MoO_2. (c) AFM image of the oxidized MoO_2. (d) Height profile along the blue arrow in (c). (For interpretation of the references to color in this figure legend, the reader is referred to the web version of this article.)

recorded in real time by a Keithley 2400 SourceMeter.

3. Results and discussion

Fig. 1b shows the scanning electron microscopy (SEM) image of the deposited MoO_2 flakes. It can be seen that all the flakes take the rhomboid shape with corner angles of 80° and 100°, respectively. The side lengths of these flakes are in the range of 2–4 μm. Raman characterization is employed to determine the crystalline structure of the sample. As shown in Fig. 1c, the Raman spectrum shows typical peaks attributed to MoO_2 at 125, 208, 229, 348, 364, 470, 497, 574, 589, and 747 cm^{-1}. These peak positions are consistent with the results obtained by Spevack et al. on MoO_2 prepared through thermal reduction of MoO_3, except a slight red shift for nearly all the peaks, which may be attributed to the differences in interfacial stress, crystal size and other related factors [10,11]. Moreover, the sharpness of Raman peaks indicates the high crystal quality of the obtained flakes.

The thicknesses of the MoO_2 flakes were determined by an atomic force microscopy (AFM). The thickness distribution of the flakes grown at sulfur temperature of 120 °C and 90 °C is shown in Fig. 2a and b, respectively. It can be seen that the thickness of the flakes shows a notable dependence on the temperature of the sulfur precursor during the growth. When the sulfur temperature is set at 120 °C, the thickness of the flakes shows a broad distribution from 6 nm to 55 nm with the peak located at the region of 15–25 nm. In contrast, the thickness of the MoO_2 flaks shows a much more narrow distribution when the sulfur temperature is set at 90 °C, with the peak located at the region of 8–9 nm. The narrow scatter of thickness distribution can also be confirmed by the similar contrast of different MoO_2 nanosheets in the optical microscopy image as shown in Fig. 2c. Fig. 2d shows the AFM topography image of the thinnest MoO_2 flakes obtained in this work. The height profile across the edge of the flake indicates that this flake is only 5.5 nm thick with the length of sides over 10 μm and an ultra-smooth surface.

We further investigated the electrical properties of the MoO_2 flakes. To evaluate the thermal stability of the obtained MoO_2 nanosheets, the samples were pre-annealed in air at 200 °C and 250 °C for 30 min on a hot plate, before the deposition of gold electrodes on top of the flakes by electron beam lithography and thermal evaporation. Fig. 3a shows the AFM image of a MoO_2 flake pre-annealed at 200 °C with pattered electrodes. Fig. 3b plots the corresponding I-V curve compared with that of a flake pre-annealed at 250 °C. The linearity of the I-V curve of the MoO_2 flake pre-annealed at 200 °C indicates that the MoO_2 is intrinsic metallic with a sheet resistance of $\sim$198 Ω/square, and the deduced electrical conductivity is 3600 S/cm. However, the sample pre-annealed at 250 °C shows an insulating behavior, implying that the MoO_2 flakes become thermal unstable at the temperature of 250 °C.

To confirm the oxidization of the MoO_2, we conducted some characterization of the MoO_2 annealed at 250 °C in air for half an hour. As shown in Fig. 4a, the color of the flakes become light blue after the thermal treatment, showing a notable color change compared to that in Fig. 2c. The sharp Raman peak located at 818 cm^{-1} (Fig. 4b) confirms that the MoO_2 flakes were oxidized into α-MoO_3 [12–15]. The topography change of the flakes after the thermal treatment was also characterized by AFM. As shown in Fig. 4c, the surface of the sample becomes much rougher, which can be seen more evidently from the height profile across the edge (Fig. 4d). We attribute this roughness to the volatility of MoO_3 at 250 °C, which creating holes in the flakes.

4. Conclusion

In summary, CVD method has been successfully employed to synthesize micrometer-sized MoO_2 nanosheets with thickness down to 5.5 nm for the first time. The concentration of the sublimated sulfur well determines the thickness distribution of the nanosheets in this work. The obtained MoO_2 nanosheets are highly crystallized into rhomboid shapes and possess atomic smooth surfaces, and exhibit high metallic conductivity with thermal stability up to 200 °C. After annealing in air at 250 °C, the MoO_2 nanosheets were oxidized into rough α-MoO_3 flakes.

Acknowledgments

This work was supported by National Natural Science Foundation of China (51472117 and 51535005), 973 Program (2013CB932604 and 2012CB933403), the Research Fund of State Key Laboratory of Mechanics and Control of Mechanical Structures (0414K01, and 0413Y02), the NUAA Fundamental Research Funds (NP2015203 and NJ20140003), Funding of Jiangsu Innovation Program for Graduate Education (KYLX15_0242), the Fundamental Research Funds for the Central Universities, and a Project Funded by the Priority Academic Program Development of Jiangsu Higher Education Institutions.

References

[1] S. Balendhran, S. Walia, H. Nili, J.Z. Ou, S. Zhuiykov, R.B. Kaner, et al., Two-dimensional molybdenum trioxide and dichalcogenides, Adv. Funct. Mater. 23 (2013) 3952–3970.

[2] S. Chuang, C. Battaglia, A. Azcatl, S. McDonnell, J.S. Kang, X. Yin, et al., MoS_2 p-type transistors and diodes enabled by high work function MoO_x Contacts, Nano Lett. 14 (2014) 1337–1342.

[3] T. Matsushima, H. Murata, Observation of space-charge-limited current due to charge generation at interface of molybdenum dioxide and organic layer, Appl. Phys. Lett. 95 (2009) 203306.

[4] L.C. Yang, Q.S. Gao, Y.H. Zhang, Y. Tang, Y.P. Wu, Tremella-like molybdenum dioxide consisting of nanosheets as an anode material for lithium ion battery, Electrochem. Commun. 10 (2008) 118–122.

[5] X.S. Wang, H.B. Feng, Y.M. Wu, L.Y. Jiao, Controlled synthesis of highly crystalline MoS_2 flakes by chemical vapor deposition, J. Am. Chem. Soc. 135 (2013) 5304–5307.

[6] T. Hao, 2D Hybrid Nanomaterials: Controllable Growth of Monolayer Molybdenum Disulphide, Degree Thesis, National University of Singapore, 2014, http://www.physics.nus.edu.sg/student/Honours%20Projects%20Repository%202013-14/Tan%20Tee%20Hao%20A0072069%20FYP%20Thesis.pdf.

[7] K.K. Wang, F.X. Wang, Y.D. Liu, G.B. Pan, Vapor growth and photoconductive property of single-crystalline MoO_3 nanosheets, Mater. Lett. 102 (2013) 8–11.

[8] S. Balendhran, J.Z. Ou, M. Bhaskaran, S. Sriram, S. Ippolito, Z. Vasic, et al., Atomically thin layers of MoS_2 via a two step thermal evaporation–exfoliation method, Nanoscale 4 (2012) 461–466.

[9] X.L. Li, Y.D. Li, Formation of MoS_2 inorganic fullerenes (IFs) by the reaction of MoO_3 nanobelts and S, Chem. Eur. J. 9 (2003) 2726–2731.

[10] P.A. Spevack, N.S. McIntyre, A. Raman, and XPS investigation of supported molybdenum oxide thin films. 1. Calcination and reduction studies, J. Phys. Chem. 97 (1993) 11020–11030.

[11] P.A. Spevack, N.S. McIntyre, Thermal reduction of molybdenum trioxide, J. Phys. Chem. 96 (1992) 9029–9035.

[12] K. Kalantar-zadeh, J.S. Tang, M.S. Wang, K.L. Wang, A. Shailos, K. Galatsis, et al., Synthesis of nanometre-thick MoO_3 sheets, Nanoscale 2 (2010) 429–433.

[13] S. Balendhran, J.K. Deng, J.Z. Ou, S. Walia, J. Scott, J. Tang, et al., Enhanced charge carrier mobility in two-dimensional high dielectric molybdenum oxide, Adv. Mater. 25 (2013) 109–114.

[14] M.A. Py, P.E. Schmid, J.T. Vallin, Raman scattering and structural properties of MoO_3, Il Nuovo Cim. B 38 (1977) 271–279.

[15] M.A. Py, K. Maschke, Intra- and interlayer contributions to the lattice vibrations in MoO_3, Phys. B+C 105 (1981) 370–374.